ISSN: 2633-4828 Vol. 5 No. S4 (July-Aug 2023)

International Journal of Applied Engineering & Technology

ENGINEERING CHITOSAN-PEG BLEND ELECTROLYTE FOR ENHANCED DSSC PERFORMANCE

Ankita Singh [1], Shivam Kashyap [2], Deepak Poddar [3], Anjana Sarkar [4*]

[1, 2, 3, 4] Department of Chemistry, Netaji Subhas University of Technology, Dwarka, New Delhi, India

[1] ankitachem17@gmail.com, [2] shivam.kashyap.phd22@nsut.ac.in,

[3]poddardeepakpoddar@gmail.com

Corresponding author*: anjana.sarkar@nsut.ac.in

Abstract

The iodine redox couple in dye-sensitized solar cells (DSSCs) functions as an electrolyte and plays a vital role by acting as an electron carrier between the photoanode and the counter electrode. Additionally, it promotes the regeneration of dye molecules by receiving electrons from the dye, thereby providing a consistent and uninterrupted flow of electrons. Iodine-based electrolytes are typically stable and exhibit excellent efficiency in electron transport under normal working circumstances. Despite its high performance, the iodine redox pair has significant drawbacks, such as corrosiveness and volatility. These drawbacks result in the degradation of the dye, hence lowering the stability and durability of the DSSC. A polymer gel electrolyte is developed using a solution approach by combining polyethylene glycol (PEG) and chitosan (Chi) in equal weight proportions. The blend is then infused with an iodine redox pair to produce an electrolyte gel for DSSC. Chitosan and PEG serve to mitigate the volatility and leakage of the iodine electrolyte by forming a barrier layer that inhibits electrolyte evaporation and shields the photoanode from corrosion induced by the iodine redox pair. The Chi-PEG is analyzed using Fourier Transform Infrared (FTIR) spectroscopy and X-ray diffraction (XRD) to determine the functional groups in the polymer electrolyte and to understand the crystalline properties of the produced polymer electrolyte, respectively. The electrolyte's thermal transition was measured using differential scanning calorimetry (DSC). The electrolyte that has been developed is then used in DSSC and exhibits comparable performance in comparison to the similar iodine redox couple polymer electrolyte.

Keywords: *Biopolymers, Polymer Gel Electrolyte, Dye-Sensitized Solar Cell, Redox Behaviour.*

INTRODUCTION

DSSCs, after their first fabrication by Gratzel in 1988, gained considerable attention owing to their ease of fabrication, high power conversion potential underneath cloudy and artificial light conditions, sustainable and inexpensive starting materials (1), low-cost fabrication to the conventional Silicon solar cells & non-hazardous nature. These cells are highly efficient in directly converting solar energy to electrical energy (2).

The working principle of a DSSC can be understood in terms of the layers it constitutes. Simple DSSC constituents of three primary layers (i) a glass sheet coated with either electrically conducting fluorine (FTO) or iodine (ITO) doped tin oxide layer, (ii) a photon absorbing layer made up of inorganic/organic semiconductors, usually TiO_2(3) soaked in a light-sensitive dye, an electrolyte generally I_2/ I_3^- redox couple to provide a media for the flow of electrons between two electrodes, and (iii) a counter electrode layer typically made up of Platinum or Graphite to facilitate the recyclability of the redox couple by collecting electrons from the external circuit(4). A large difference within the Fermi levels between the photoanode and counter electrode beneath illumination can exhibit an outsized potential difference, thus facilitating a large current to be delivered by the device.

Though I_2/ I_3^- couple extensively as an electrolyte in DSSC and has multiple functions. Iodine electrolytes work in synergism with both the photoanode and the counter. The electrolyte goes deep inside the photoanode material, promoting mobility and acting as a hole transport material (5). It also helps regenerate the Dye molecule's oxidized state after the electrons from the excited state are injected into the conduction band of the photoanode during illumination. I_3^- transferring electrons from the counter helps to hold back any overpotential caused by the accumulation of electrons at the counter electrode (6). Although widely used, the electrolyte has many drawbacks

associated with it, which include sealing issues faced during the use of liquid electrolytes in general, inflammability, corrosion of electrical contacts by the triiodide/Iodide redox couple (for example, the corrosion of silver-based current collectors) (7) and the partial absorption of visible light around 430 nm by the triiodide species thus limits its scale up to the size of the module (8).

$$I^- + I_2 \leftrightarrow I_3^- \leftrightarrow I_5^-$$

$$3I^- + 2D^+ \rightarrow I_3^- + 2D(photoanode)$$

$$I_3^- + 2e^- \leftrightarrow 3I^-(counterelectrode)$$

To overcome this, looking for alternatives that can play the role of iodine electrolytes without compromising the device's efficiency becomes essential. This is where the gel polymer electrolytes come into the picture. The electrolyte membrane of polymers can be used as an ionic conductor in DSSCs in place of liquid electrolytes (9). The electrolytes based on the polymers help resolve the issues relating to inflammability, leaking, and sealing of the device and provide flexibility to the unit. These also provide electrochemical stability lacking by the conventional iodine electrolyte (10). Solid polymer electrolytes are disadvantageous as the ionic conductivity is very low compared to liquid electrolytes, and thus, attention should be given to gel polymer electrolytes with higher ionic conductivity than solid polymer electrolytes (11).

Chitosan (β-1,4-D-glucosamine) is a widely used natural polymer owing to its ionic conductivity and abundant availability, mostly from fisheries Industries' waste. Chitosan easily solubilizes in a weakly acidic solution of protic solvents, and the dissolution forms a positively charged (cationic) polymer (12). This highly charged Chitosan can thus form polyelectrolyte complexes with a vast range of anionic polymers. The polymers consist of both the crystalline and amorphous phases. The inorganic salts, such as NH_4I, KI, etc., increase the amorphous character of the polymers, so the motion of ions occurs in a more accessible manner. Li^+ ions, due to their small size, can quickly move along in the polymer matrix**.** Also, the energy required for dissociating LiI in its ions is low, and the process could be easily carried out at RT (13)**.** Thus. LiI/I_2 is the most commonly used electrolyte system for dye-sensitized solar cells**.**

In the present work, a polymeric blend of Chitosan and PEG containing LiI/I_2 to generate the redox couple to enhance the ionic conductivity of the electrolyte has been prepared, where the Chi-PEG blend acts as a matrix. Using a Chi-PEG blend as an electrolyte based on Li-ion has shown conductivity as high as 10^{-6} S/cm at room temperatures (6). The synthesized polymer gel electrolyte is characterized by Fourier Transform Infrared Spectroscopy (FTIR) to account for the linkages of various functional groups in the polymer blend, UV-Visible Spectroscopy, the change in crystallinity was studied by performing X-ray diffraction (XRD) and differential scanning calorimetry (DSC) studies on the polymer blend and the insights of the structural changes were seen through Scanning Electron Microscopy (SEM) and conductivity of polymer blend was calculated by measuring its I-V characteristics through electrometer.

The fabrication polymer electrolyte was then used in the solar cell device, and the corresponding J-V characteristics were obtained based on which the efficiency of the cell was calculated.

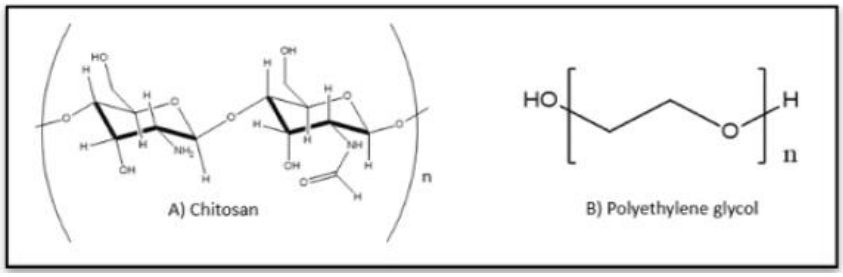

Figure 1. Chemical structure of a) Chitosan and b) PEG.

MATERIALS AND EXPERIMENTS

A. Materials:

Chitosan (50-190kDa, 85% degree of deacetylation and viscosity of 20-300 cPs), PEG-4000, Sodium molybdate & Selenium powder were purchased from CDH chemicals. All other chemicals used in the device fabrication were bought from Merck. The purchased chemicals were used as it is without any further purification.

B. Methods

a. Preparation of Electrolyte

The blend was prepared by dissolving 2%(w/v) chitosan in 1 % glacial acetic acid (AA) aqueous solution. To achieve a clear solution, a similar weight of PEG as that of chitosan was added to the above solution, and the whole blending process was carried out at 40^{o}C until a clear solution was obtained. All the prepared concentrations of LiI/I_2 solutions, as mentioned in Table-1, were added to the blends separately, appropriately mixed, and then the blend was poured into the Petri dish and subjected to vacuum drying at 40^{o}C for 24h to remove any of the entrapped bubbles to obtain the dry film and stored under vacuum at room RT for further use.

Table I: Contains the concentrations used in the preparation of polymer electrolytes.

S.No.	Weight of Chitosan and PEG in AA	Volume of Electrolyte used	LiI	I_2	Temperature of study
	(w/v) %	(v/v) %	(mM)	(mM)	(^{o}C)
1	2	20	0	0	40
2	2		100	10	
3	2		200	20	
4	2		300	30	
5	2		400	40	
6	2		500	50	

b. Preparation of DSSC

Photo anode: A homogeneous layer of TiO_2 was deposited on the conducting side of FTO by the widely used Doctor's blade method, and then the FTO was annealed at 350^{o}C for 30 min.

Sensitization of Photo Anode: The annealed photo Anode was sensitized in the $3x10^{-4}$ M ethanol solution of N3 dye for 24 hours. Afterward, the sensitized anode was washed with distilled water and ethanol to remove loosely attached dye and dried at 60^{o}C for 1hr.

Counter Electrode: The standard platinum electrode is fabricated by drop casting 10µl of the 5mM solution of 8% (w/v) of H_2PtCl_6 on pre-cleaned FTO and then heating the FTO at 350^{o}C for 1h.

c. Device fabrication and study:

Dye-sensitized Titanium-based photoanode and Pt counter electrode are sandwiched, and the polymer gel electrolyte is poured from the side of FTO. The fabricated cell was illuminated with an LED lamp, and corresponding I-V characteristics were recorded against variable resistance. Based on the obtained data, the graph showing the I-V characteristics of the device is plotted. The efficiency was calculated by using equations 1,2 and 3:

$$FF = \frac{I_m V_m}{I_{sc} V_{sc}} \quad \text{(Equation 1)}$$

$$FF(\%) = \frac{I_m V_m}{I_{sc} V_{sc}} \times 100$$ (Equation 2)

$$\eta = \frac{I_{mp} V_{mp}}{J \cdot S}$$ (Equation 3)

Where,

FF = fill factor indicative of square ness of the V-I curve in the solar cell characteristics

J = Intensity of the Light source used

S = Active Surface area of the device

I_{sc} & V_{sc} = Short circuit current and voltage offered by the device

d. Characterization study:

The absorbance of the prepared electrolyte (500µl in 3ml of 2% AA solution) was measured in the range of 190cm-1100cm against distilled water as a reference using Esico-International's double beam UV-Vis Spectrophotometer. FTIR spectra for all the films were recorded by making the pellet of the ground film with KBr, and then the pellet was scanned between the frequency range of 4250 cm^{-1} - 400 cm^{-1} in the attenuated total reflection (ATR) mode on Spectrum RXI spectrometer spectrophotometer with a resolution of 1 cm^{-1}.

For the morphological study, an optical microscope from Zeiss 420 and the scanning electron micrographs (JSM-7900F Prime Field Emission SEM model from JEOL) have been used to obtain the surface images of the polymer electrolyte. X-ray diffraction studies were conducted at 2º/min for the scan angle range of 5º-80º at 30kV and 15mA. on the Bruker D8 Discover diffractometer (Cu Kα radiation) to evaluate the Physicochemical properties of the polymer electrolyte.

RESULTS AND DISCUSSION

A. Fourier transform Infrared spectroscopy (FTIR) study.

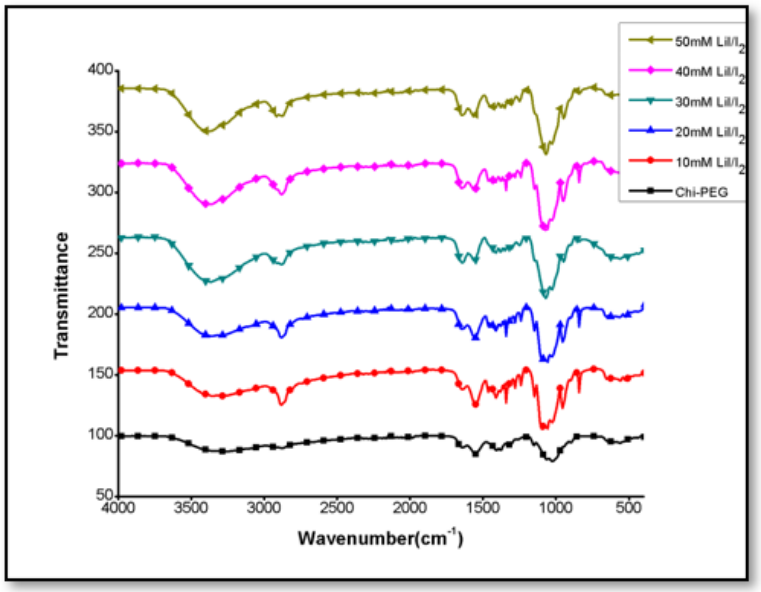

Figure 2. FTIR spectra of Chi-PEG and blend containing 10mM, 20mM, 30mM, 40mM, and 50mM of the redox couple LiI/I2, as mentioned in Table 1.

The FTIR spectra recorded for pure chitosan shows absorption peaks for OH stretching (3358cm^{-1}), CH stretching (2923 cm^{-1}), amide i.e., C=O stretching (1650 cm^{-1})(14) amide II for NH bending (1580 cm^{-1}), CH_3 stretching (1385 cm^{-1}) and C-O stretching (1033 cm^{-1}) whereas absorption peak for PEG is observed for 2886 cm^{-1}, 1470 cm^{-1}, 1350 cm^{-1}, 1283 cm^{-1}, 955 cm^{-1} and 841 cm^{-1} (15).

In the chitosan and PEG blend, there is no addition or elimination of characteristic peaks of chitosan and PEG, suggesting no chemical reaction has occurred (16). With the addition of aqueous LiI/I_2, it is observed that

(i) The broad band at 3340 cm^{-1} in the blend shifts to a higher wave number due to the hygroscopic nature of the lithium salt, and the band intensifies with the increase in concentration. This is due to the interaction of positively charged Li ions with the carbonyl group (17).

(ii) The N-H bending vibration at 1595 cm^{-1} in the blend shifts to a higher wavenumber showing that the amide group is affected by adding iodine to the blend.

(iii) The shift of IR frequency at 1061 cm^{-1} characteristic for C-O stretching towards the lower wavenumber is due to the interaction of iodine with the positively charged amino group in the blend (14).

FTIR results indicate the interaction of iodine with the chitosan, which can be proved by the shifting of the above-mentioned peaks.

B. X-ray Diffraction (XRD) study

Pure chitosan shows a strong reflection around 20^{o} and a weaker reflection at 10^{o}, showing its crystalline nature. Pure PEG shows strong reflection at 19^{o} and 23^{o} and weaker reflection at 27^{o}, 30.5^{o}, 36^{o}, and 40^{o}, which shows the crystalline nature of PEG. On blending Chi-PEG in the ratio 1:1, the observed XRD pattern is devoid of any crystalline peak observed in the case of pure chitosan and PEG but observes a broad peak at 22.5^{o} which shows reduced crystallinity of both chitosan and PEG (18).

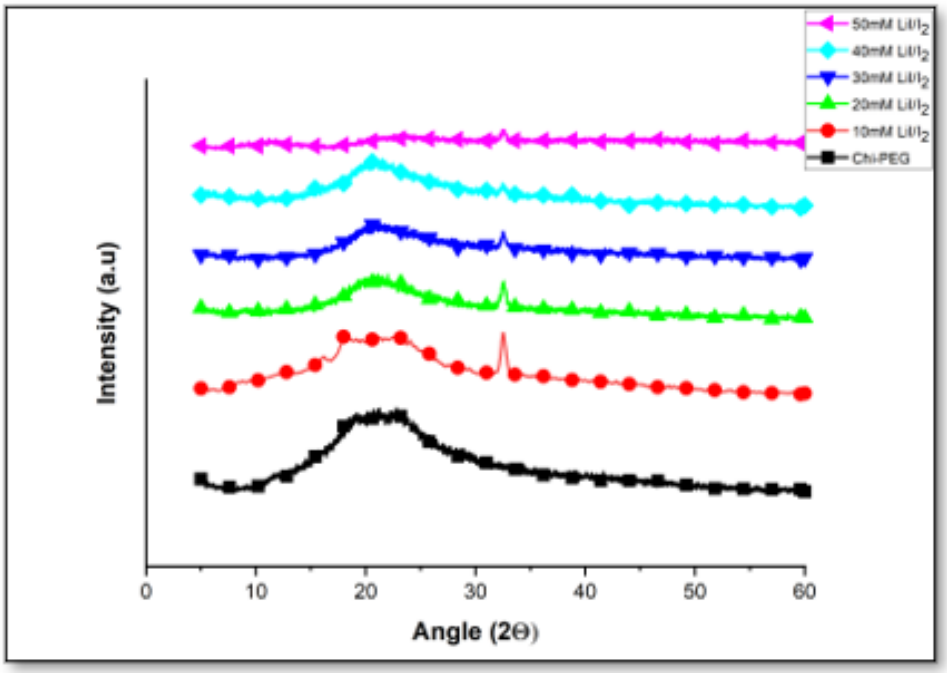

Figure 3. XRD pattern of the Chi-PEG blend with varied LiI/I2 redox couple concentrations.

The crystallinity is further reduced by adding LiI/I_2 to the blend, which is seen from the reduced intensity of the broad peak at 19^{o}-23^{o} (19). A new peak was introduced at 32.5^{o} with the addition of aqueous LiI/I_2 in the blend

system, which may be due to the interaction of iodine with the amino group of the chitosan. This interaction first introduces some crystallinity to the blend system, which is later reduced by adding a higher concentration of the redox couple. This behavior of the blend system has also been proven by DSC results.

C. Differential scanning calorimetry

DSC measurements have been performed in double cycles under the continuous nitrogen gas supply. Although there are various crystalline regions present in its structure, chitosan does not show any thermal transition, which can be understood in terms of intra and intermolecular bonding, which builds the rigid structural backbone of Chi (20).

Table II: Enthalpy of crystallization for the blend and blend with different concentrations of the redox couple.

S. No.	Electrolyte	T_m	ΔH (J/g)	Crystallinity (%)
1	PEG	53.66	42.56	49.6
2	blend	58.71	60.38	70.4
3	0.1M	61.04	73.29	85.4
4	0.2M	55.18	71.61	83.4
5	0.3M	52.75	63.53	74.0
6	0.4M	51.60	28.33	33.0
7	0.5M	50.50	25.98	30.2

Figure 4 shows the dip at 53.6^{O}C ascribed to the melting (T_m) of PEG, which shifts to a lower temperature with the addition of chitosan in the blend; this may have occurred due to the crystalline nature of chitosan, and as chitosan was added in the blend it acts as a nucleating agent as results in the T_m might shift towards the higher value which was calculated using the equation 4 in table 3. The area under the DSC curve provides insights into the crystalline nature of the sample, and the decreasing area points towards the reduction in crystallinity of the polymer blend, which is calculated by:

$$\% \text{ Crystallinity} = \left(\frac{\Delta Hexp}{\Delta Hth}\right) x\ 100 \qquad \text{(Equation 4)}$$

With the addition of aqueous LiI/I_2, the depth of the hump in the curve decreases, and a lowering in the temperature is observed, which suggests the enhancement in the amorphous nature of the electrolyte. At initial, low concentration of the LiI/I^2 acts as a nucleating agent, which enhances the crystal growth of PEG. As a result, the T_m was increased from 58.71 to 61.04^{O}C, but as the concentration of electrolyte increased, the plasticization phenomenon was also introduced to the blend, due to which PEG shows a decrease in T_m as well as in % crystallinity, but the ionic conductivity of the electrolyte enhances.

D. UV-Visible Spectroscopy

Absorption characteristics of the LiI/I^2 redox coupled with chitosan-PEG blend in different ratios are shown in Figure 4. Pure chitosan and PEG show no significant peaks in UV-vis spectra due to the absence of any chromophore group in the backbone of these polymer backbone chains. The three-absorption peak appeared at 240, 288, and 350nm as the redox couple was added to the blend.

This broadening and appearance of multiple peaks can be attributed to the enhancement in the absorption of light, which harvests the broader spectrum of solar energy and can be beneficial in producing higher photocurrent. The recorded spectra show increasing peak intensity with the increased concentration of the redox couple, as was expected.

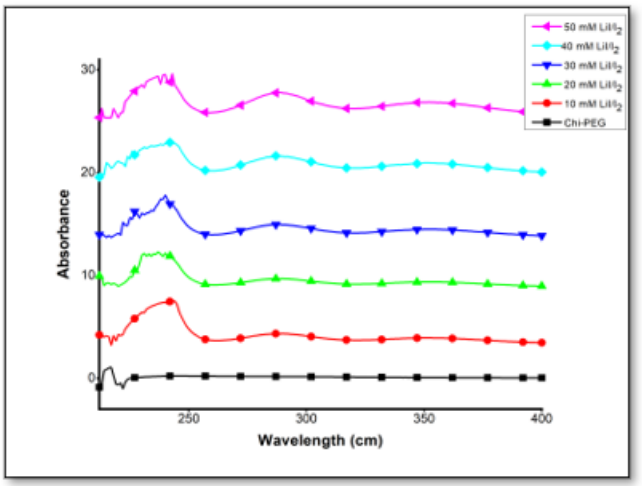

Figure 4. The absorption pattern of the polymer blend with different concentrations of LiI/I_2 used.

E. Scanning Electron Microscopy

Figure 5 depicts the scanning electron micrographs obtained by Scanning coated samples of the polymer electrolyte. Figure 5A shows the smooth morphology of the blend. Figure 5 shows the SEM micrographs obtained for the polymer electrolyte containing different concentrations of LiI/I_2 and homogeneous without any phase separation, which signifies the presence of intermolecular interaction between both phases. The morphology tended to move toward the surface roughness and porosity with the addition of iodine redox couple. The number of micro-pores appearing on the film's surface increases with the higher dosage of iodine redox couple solution due to the disturbed crystal structure in the blend. This is attributed to the increased amorphous nature, as the XRD & DSC curves also support. The migration of ions thus becomes more relaxed with the amorphous nature of the polymer electrolyte (21)**.**

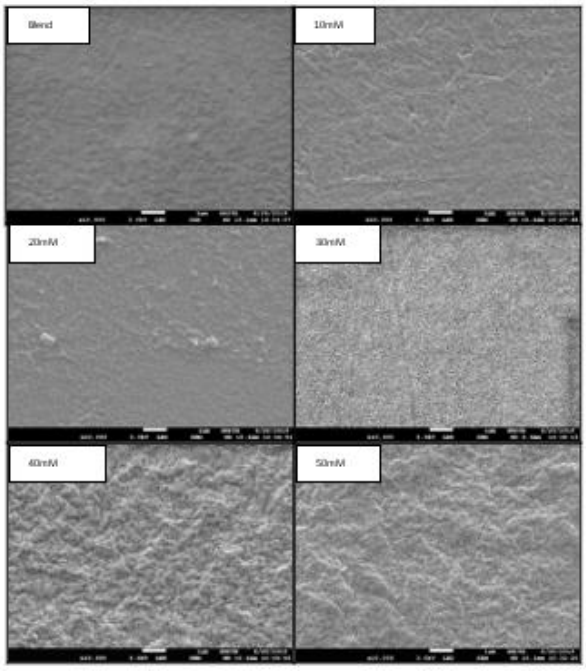

Figure 5. SEM images of the blend and fabricated polymer film with different electrolyte concentrations.

F. Conductivity Measurement

The I-V Characteristics of the polymer gel electrolyte were measured with the help of a 6517B Electrometer/High resistance meter at room temperature. The graph is recorded between the current obtained and voltage applied at -/+30 volts. The straight line thus obtained provides agreement with the Ohm law(22).

It is observed that with the increasing concentration of the Li/I redox couple in the polymer blend, the current also increases. Based on the current obtained in the Gel Polymer electrolyte, the highest concentration is used to fabricate the DSSC device.

I-V characteristics show a steep slope in the case of the 0.5 M concentration of gel polymer electrolyte and reveal a considerable current. Thus, the device fabrication is sought to use the highest concentration i.e., 0.5M. Also, two other concentrations of only blend and 0.3M have been used in the cell fabrication to observe the effect of electrolyte concentration.

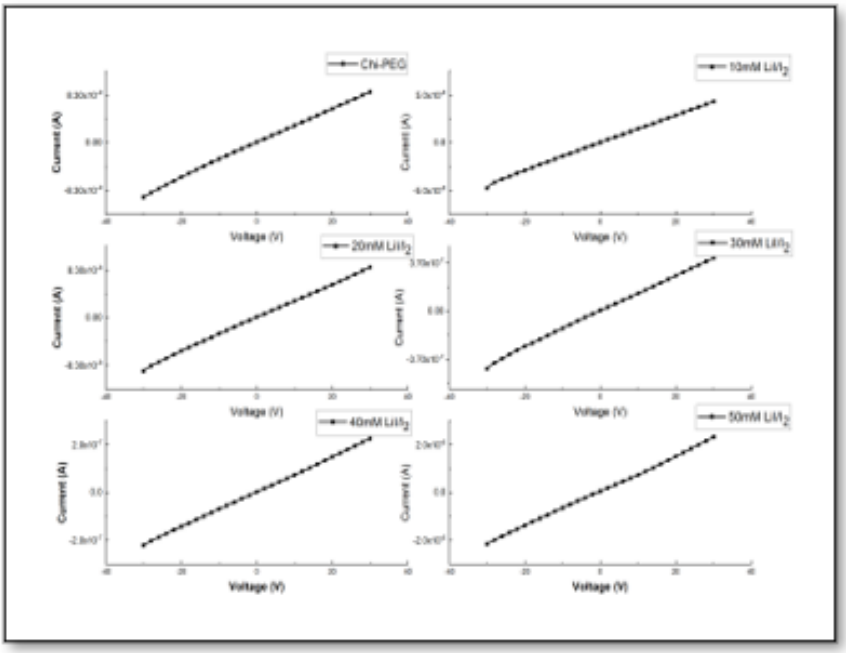

Figure 6. Conductivity of the fabricated polymer film with different electrolyte concentrations.

G. Working of Device:

The device fabricated by the method already discussed above was tested under the illumination of an LED lamp placed at a working distance of 25 cm from the device. The current and voltage generated for the particular intensity were recorded using a primary electric circuit involving multimeters or required values. Figure 7 shows the solar cell characteristics graph and Table (3) summarizes the parameters obtained from it. The high conductivity values of the biopolymer-salt complexed systems further confirm that biopolymer electrolyte could be a novel alternative in the development of highly efficient DSSC and batteries and aid the scientific community in maintaining a clean and environmentally friendly environment (23).

Table III: Solar cell characteristics obtained for Chi-PEG with 50mM LiI/I_2 concentration.

Electrolyte system	V_{oc}	I_{sc}	V_m	I_m	P_{max}	ff	n
Chitosan-PEG	412	2.62	242	2.22	537.24	0.5	1.07

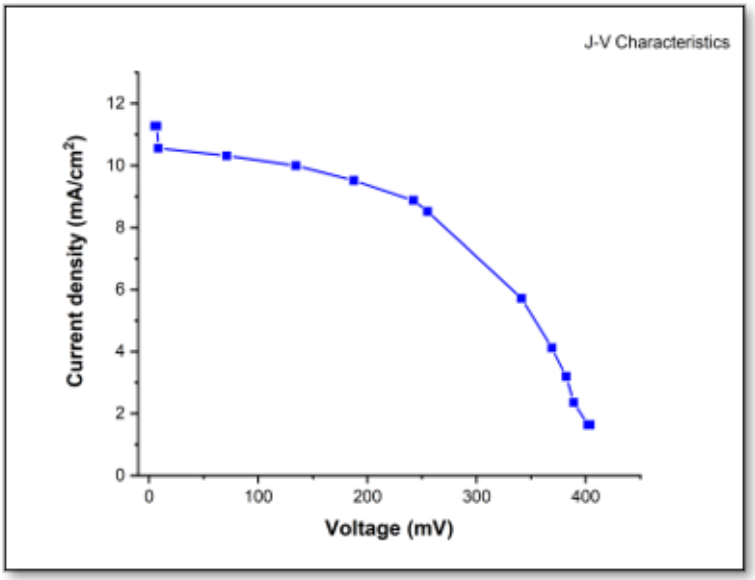

Figure 7. J-V characteristics obtained for the device fabricated with 50mM LiI/I_2.

CONCLUSION

Li^+/ I_3^- has been the most commonly used electrolyte system while working with the dye-sensitized solar cell. Due to leakage problems faced with the working of liquid electrolytes, the LiI/I_2 system can be used with the polymer matrix known as gel polymer electrolyte.

The present study uses a matrix of LiI/I_2 redox coupled with the Chitosan-PEG blend System. A morphological study showed the increased amorphous nature of the electrolyte, which is also supported by the thermal data obtained by DSC, where the reduction in crystallinity percentage was observed, as well as the XRD data. At first, crystallinity increased while moving from Pure PEG to the blend system, but with the increased concentration of redox couple, a decrease in the percentage of crystallinity was observed. The conductivity of the polymer electrolyte is significantly affected by the concentration of the redox couple.

The device fabricated has been tested with the variable resistance method under a similar degree of Intensity which showed an efficiency of 1. 07 %.

REFERENCES

[1] Su'Ait MS, Ahmad A, Badri KH, Mohamed NS, Rahman MYA, Ricardo CLA, et al. The potential of polyurethane bio-based solid polymer electrolyte for photoelectrochemical cell application. In: International Journal of Hydrogen Energy. 2014. p. 3005–17.

[2] Gong J, Liang J, Sumathy K. Review on dye-sensitized solar cells (DSSCs): Fundamental concepts and novel materials. Vol. 16, Renewable and Sustainable Energy Reviews. 2012. p. 5848–60.

[3] Arof AK, Buraidah MH, Teo LP, Majid SR, Yahya R, Taha RM. Characterizations of chitosan-based polymer electrolyte photovoltaic cells. International Journal of Photoenergy. 2010;2010.

[4] Yuan X, Zhou B, Zhang X, Li Y, Liu L. Hierarchical MoSe2 nanoflowers used as highly efficient electrode for dye-sensitized solar cells. Electrochim Acta. 2018 Sep 1; 283:1163–9.

[5] Shozo Y, Youhai Y, Kazuhiro M. Iodine/iodide-free dye-sensitized solar cells. Acc Chem Res. 2009 Nov 17;42(11):1827–38.

[6] Cao F, Oskam G, Searson PC. A Solid State, Dye Sensitized Photoelectrochemical Cell [Internet]. Vol. 99, J. Phys. Chem. 1995. Available from: https://pubs.acs.org/sharingguidelines

[7] Philippi F, Rauber D, Zapp J, Prãsang C, Scheschkewitz D, Hempelmann R. Multiple ether-functionalized phosphonium ionic liquids as highly fluid electrolytes. ChemPhysChem. 2019;20(3):443–55.

[8] Wang M, Chamberland N, Breau L, Moser JE, Humphry-Baker R, Marsan B, et al. An organic redox electrolyte to rival triiodide/iodide in dye-sensitized solar cells. Nat Chem. 2010 May;2(5):385–9.

[9] Li Q, Tang Q, Du N, Qin Y, Xiao J, He B, et al. Employment of ionic liquid-imbibed polymer gel electrolyte for efficient quasi-solid-state dye-sensitized solar cells. J Power Sources. 2014; 248:816–21.

[10] Zhang C, Kazanci OB, Levinson R, Heiselberg P, Olesen BW, Chiesa G, et al. Resilient cooling strategies – A critical review and qualitative assessment. Energy Build. 2021 Nov 15;251.

[11] Su'ait MS, Rahman MYA, Ahmad A. Review on polymer electrolyte in dye-sensitized solar cells (DSSCs). Solar Energy. 2015 May 1; 115:452–70.

[12] Singh R, Polu AR, Bhattacharya B, Rhee HW, Varlikli C, Singh PK. Perspectives for solid biopolymer electrolytes in dye sensitized solar cell and battery application. Vol. 65, Renewable and Sustainable Energy Reviews. Elsevier Ltd; 2016. p. 1098–117.

[13] Cao X, Li H, Li G, Gao X. Electrocatalytically active MoSe 2 counter electrode prepared in situ by magnetron sputtering for a dye-sensitized solar cell [Internet]. Vol. 40, Chinese Journal of Catalysis. 2019. Available from: http://www.sciencedirect.com/science/journal/18722067

[14] Limchoowong N, Sricharoen P, Techawongstien S, Chanthai S. An iodine supplementation of tomato fruits coated with an edible film of the iodide-doped chitosan. Food Chem. 2016 Jun 1; 200:223–9.

[15] Chieng BW, Ibrahim NA, Yunus WMZW, Hussein MZ. Poly (lactic acid)/poly (ethylene glycol) polymer nanocomposites: Effects of graphene nanoplatelets. Polymers (Basel). 2014;6(1):93–104.

[16] He LH, Xue R, Yang DB, Liu Y, Song R. Chinese Journal of Polymer Science EFFECTS OF BLENDING CHITOSAN WITH PEG ON SURFACE MORPHOLOGY, CRYSTALLIZATION AND THERMAL PROPERTIES * [Internet]. Vol. 27, Chinese Journal of Polymer Science. 2009. Available from: www.worldscientific.com

[17] Che Balian SR, Ahmad A, Mohamed NS. The effect of lithium iodide to the properties of carboxymethyl κ-carrageenan/carboxymethyl cellulose polymer electrolyte and dye-sensitized solar cell performance. Polymers (Basel). 2016;8(5).

[18] Kolhe P, Kannan RM. Improvement in Ductility of Chitosan through Blending and Copolymerization with PEG: FTIR Investigation of Molecular Interactions. 2003;

[19] Li Y, Dong S, Chen B, Lu C, Liu K, Zhang Z, et al. Li-O2 Cell with LiI(3-hydroxypropionitrile)2 as a Redox Mediator: Insight into the Working Mechanism of I- during Charge in Anhydrous Systems. Journal of Physical Chemistry Letters. 2017 Sep 7;8(17):4218–25.

[20] Gunbas ID, Aydemir Sezer U, Gülce I S, Deliloğlu Gürhan I, Hasirci N. Semi-IPN chitosan/PEG microspheres and films for biomedical applications: Characterization and sustained release optimization. Ind Eng Chem Res. 2012 Sep 19;51(37):11946–54.

[21] Rani MSA, Rudhziah S, Ahmad A, Mohamed NS. Biopolymer electrolyte based on derivatives of cellulose from kenaf bast fiber. Polymers (Basel). 2014;6(9):2371–85.

[22] Huo Z, Wang L, Tao L, Ding Y, Yi J, Alsaedi A, et al. A supramolecular gel electrolyte formed from amide based co-gelator for quasi-solid-state dye-sensitized solar cell with boosted electron kinetic processes. J Power Sources. 2017; 359:80–7.

[23] Singh R, Polu AR, Bhattacharya B, Rhee HW, Varlikli C, Singh PK. Perspectives for solid biopolymer electrolytes in dye sensitized solar cell and battery application. Vol. 65, Renewable and Sustainable Energy Reviews. Elsevier Ltd; 2016. p. 1098–117.